PRESYNAPTIC CALCIUM DIFFUSION FROM VARIOUS ARRAYS OF SINGLE CHANNELS

Implications for Transmitter Release and Synaptic Facilitation

AARON L. FOGELSON AND ROBERT S. ZUCKER
Departments of Mathematics and Physiology-Anatomy, University of California, Berkeley, California 94720

ABSTRACT A one-dimensional model of presynaptic calcium diffusion away from the membrane, with cytoplasmic binding, extrusion by a surface pump, and influx during action potentials, can account for the rapid decay of phasic transmitter release and the slower decay of synaptic facilitation following one spike, as well as the very slow decline in total free calcium observed experimentally. However, simulations using this model, and alternative versions in which calcium uptake into organelles and saturable binding are included, fail to preserve phasic transmitter release to spikes in a long tetanus. A three-dimensional diffusion model was developed, in which calcium enters through discrete membrane channels and acts to release transmitter within 50 nm of entry points. Analytic solutions of the equations of this model, in which calcium channels were distributed in active zone patches based on ultrastructural observations, were successful in predicting synaptic facilitation, phasic release to tetanic spikes, and the accumulation of total free calcium. The effects of varying calcium buffering, pump rate, and channel number and distribution were explored. Versions appropriate to squid giant synapses and frog neuromuscular junctions were simulated. Limitations of key assumptions, particularly rapid nonsaturable binding, are discussed.

INTRODUCTION

The brief duration of transmitter release and the longer facilitation of release by subsequent action potentials have been attributed to the diffusion of calcium away from the presynaptic plasma membrane after influx during a spike (Zucker, 1982; Zucker and Stockbridge, 1983; Stockbridge and Moore, 1984; Zucker, 1985*a*). Such a calcium diffusion model has been extended to account for both synaptic facilitation and the accumulation of total presynaptic calcium as measured spectrophotometrically during and after a tetanus (Zucker, 1984, 1985*b*). However, this model incorrectly predicts a great prolongation of phasic transmitter release evoked by late spikes in a tetanus due to the accumulation of a residual "active," or submembrane, calcium that reaches too high a level compared to the peak active calcium in a single spike.

In this model, calcium enters uniformly through the surface membrane and diffuses radially in one dimension. This formulation fails to recognize that calcium actually enters through discrete channels, leading to pronounced nonuniformities in the submembrane calcium concentration at the end of a spike (Simon et al., 1984; Chad and Eckert, 1984). Diffusion away from channel mouths is slowed to ~0.01 $\mu m^2/ms$ by the rapid binding of >95% of calcium in cytoplasm (Brinley, 1978). This allows calcium to diffuse only ~50 nm in the 200 μs between the peak of calcium influx in a spike and the beginning of transmitter release (Llinás, 1977). Release must occur near channel mouths before diffusional equilibration can occur at the surface. The peak active calcium concentration must therefore be substantially higher than indicated by the one-dimensional diffusion model. A more realistic model might predict a more rapid decay of active calcium and phasic release, even in late spikes in a tetanus, while leaving the time courses of residual calcium, facilitation, and total presynaptic calcium unaffected. To test these ideas, we have developed a three-dimensional calcium diffusion model, in which calcium enters through discrete channels and diffuses internally in three dimensions from channel mouths to nearby release sites.

METHODS

One-Dimensional Model

To simulate presynaptic calcium movements at squid giant synapses, we solved the diffusion equation in cylindrical coordinates. It was assumed that calcium enters uniformly through the whole surface membrane of the terminal and diffuses only in a radial direction (i.e., longitudinal and circumferential gradients were assumed to be negligible). Diffusion was slowed from its value in aqueous solution ($D = 0.6\ \mu m^2/ms$) by rapid binding to uniformly distributed fixed binding sites, with a ratio of bound to free calcium (β) of 40 (Brinley, 1978). A boundary condition at the surface included terms for the influx of calcium during action potentials and at rest, and its removal by a first-order pump. The pump rate (P) was set to 0.08 $\mu m/ms$ to remove calcium from cytoplasm at a rate similar to that observed experimentally at squid giant synapses (Charlton et al., 1982). Resting calcium influx was set to 40 fM/cm^2-s, resulting in a resting free calcium level of 20 nM (DiPolo et al., 1976). Calcium influx during action potentials was represented by a 1-ms square pulse of 1

nM/cm²-s, corresponding to an inward calcium current of ~210 nA for 1 ms in a terminal 700 μm long and 50 μm in diameter (Llinás et al., 1982). Stockbridge and Moore (1984) have shown that this approximation to the time course of calcium current yields results similar to those obtained using a more accurate representation of the calcium current.

The diffusion equation was evaluated numerically by finite-difference methods. A submembrane shell thickness of 100 nm was used, which gave results within 10% of those obtained using 10-nm shells. Details of this model have been published previously (Zucker and Stockbridge, 1983). The previous publication contained an error in Eq. 4: the terms for pumping (P) and influx (J_{in}) must be divided by $(1 + \beta)$ to account for the effect of cytoplasmic calcium binding on extrusion and the fraction of entering calcium that remains free. In the earlier paper, implicit or backwards difference methods (Moore et al., 1975) were used to solve the finite difference equations with relatively large time and distance steps. In the present simulation, the finite difference equations were solved explicitly, to more easily accommodate nonlinear (saturating) binding and pumping.

Three-Dimensional Model

In this model, calcium enters the presynaptic terminal through an array of discrete channels. As in the one-dimensional model, calcium is rapidly bound to immobile, nonsaturable cytoplasmic sites and calcium is extruded at the terminal's surface. We represented the terminal as a cylinder with rectangular cross-section, with the channels grouped in thousands of discrete active zone patches on the terminal's synaptic face (Fig. 1 *A* and *B*). We considered the movement of calcium in a rod-like element extending through the terminal and with one end containing a patch of channels (Fig. 1 *C*). The sides of this element are the boundaries between adjacent elements of the terminal. By symmetry, there is no net diffusion of calcium across these boundaries.

Let $c(x, y, z, t)$ be the concentration change above resting level of free calcium at a point in the element. Then the equations of our model are

$$\frac{\partial c}{\partial t} = \frac{D}{(1 + \beta)} \nabla^2 c \tag{1}$$

$$D \frac{\partial c}{\partial y} + Pc = f(x, z)\, g(t), \text{ at } y = y_0 \tag{2}$$

$$-D \frac{\partial c}{\partial y} + Pc = 0, \text{ at } y = -y_0 \tag{3}$$

$$\frac{\partial c}{\partial x} = 0, \text{ at } x = \pm x_0 \tag{4}$$

$$\frac{\partial c}{\partial z} = 0, \text{ at } z = \pm z_0 \tag{5}$$

$$c(x, y, z, 0) = 0 \tag{6}$$

$$R(x, z, t) = k\, c(x, y_0, z, t)^n \tag{7}$$

Here, D, P, and β represent the same parameters as in the one-dimensional model. The function $g(t)$ describes the time course of calcium influx through the channels and is usually taken to be a train of square pulses. The function $f(x, z)$ describes the distribution of channels on the synaptic face, $y = y_0$, of the element. Since the channels are much smaller than the patch, $f(x, z)$ is effectively a sum of delta-like functions centered on the channels. The factor $1/(1 + \beta)$ appears in Eq. 1 because only the free calcium can diffuse. Eqs. 2 and 3 reflect the balance of calcium fluxes at the surface membrane, and Eqs. 4 and 5 express the absence of diffusion across the sides of the element. The function R in Eq. 7 is the rate of transmitter release, and therefore the amplitude of the postsynaptic response; we assume it is proportional to a prescribed power of the submembrane free calcium concentration at selected points near

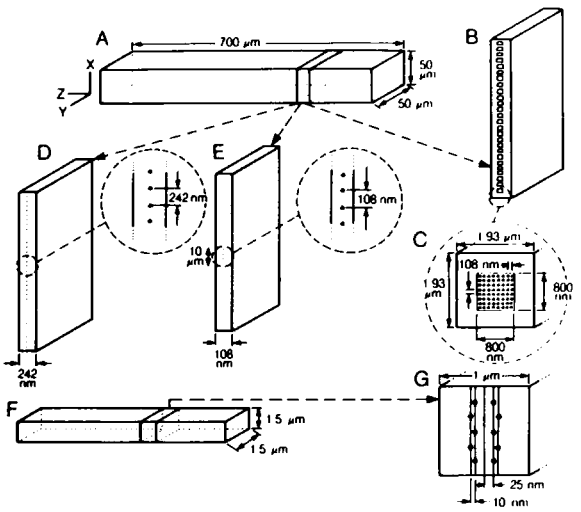

FIGURE 1 Unit elements of presynaptic terminal in which diffusion equation was solved in three-dimensional model. (*A*) Rectilinear cylinder representing squid terminal and showing coordinate system. (*B*) Slice of terminal, with 26 active zones in a row in the synaptic face. (*C*) Element of terminal, containing one active zone. (*D*) Element of terminal for simulations in which calcium channels are dispersed uniformly throughout synaptic face. (*E*) Element of terminal for simulations in which calcium channels are concentrated in a central strip of the synaptic face. (*F*) Rectilinear cylinder representing frog motor neuron terminal. (*G*) Element of terminal containing one active zone. In *C–E* and *G*, the dots represent calcium channels, and release sites are 50 nm from channel mouths.

the calcium channels (active calcium). Eqs. 1 to 6 may be solved for $c(x, y, z, t)$ by separation of variables and superposition, using Duhamel's Principle to go from the solution for a time-independent calcium influx, $g(t) = 1$, to that for the time-dependent case (Berg and McGregor, 1966). The most immediate form of the solution obtained in this way is

$$c(x, y, z, t) = \frac{1}{1 + \beta} \cdot \int_0^t g(\tau)\, S_1(y, t - \tau)\, S_2(x, z, t - \tau) \mathrm{d}\tau, \tag{8}$$

where

$$S_1(y, t - \tau) = \sum_{l=1}^{\infty} \left\{ \frac{\left[\omega_{1l}^2 + \frac{P^2}{D^2}\right] \cos(\omega_{1l} y_0) \cos(\omega_{1l} y)}{\left(y_0 \left[\omega_{1l}^2 + \frac{P^2}{D^2}\right] + \frac{P}{D}\right)} \cdot e^{[-D\omega_{1l}^2 (t-\tau)]/(1+\beta)} + \frac{\left[\omega_{2l}^2 + \frac{P^2}{D^2}\right] \sin(\omega_{2l} y_0) \sin(\omega_{2l} y)}{\left(y_0 \left[\omega_{2l}^2 + \frac{P^2}{D^2}\right] + \frac{P}{D}\right)} \cdot e^{[-D\omega_{2l}^2 (t-\tau)]/(1+\beta)} \right\}, \tag{9}$$

$$S_2(x, z, t-\tau) = \sum_{n=0}^{\infty}\sum_{k=0}^{\infty} a_{nk} \cos\left(\frac{n\pi z}{z_0}\right) \cdot \cos\left(\frac{k\pi x}{x_0}\right) e^{[-D\pi^2\gamma_{nk}^2(t-\tau)]/(1+\beta)}, \quad (10)$$

$$\gamma_{nk}^2 = \frac{n^2}{z_0^2} + \frac{k^2}{x_0^2}, \quad (11)$$

ω_{1l} and ω_{2l}, $l = 1, 2, 3, \ldots$ are, respectively, the positive solutions of

$$\frac{D\omega_{1l}}{P} = \cot(\omega_{1l} y_0) \text{ and } \frac{-D\omega_{2l}}{P} = \tan(\omega_{2l} y_0), \quad (12)$$

and

$$f(x, z) = \sum_{n=0}^{\infty}\sum_{k=0}^{\infty} a_{nk} \cos\left(\frac{n\pi z}{z_0}\right)\cos\left(\frac{k\pi x}{x_0}\right). \quad (13)$$

The series $S_2(x, y, t, \tau)$ converges very slowly, especially for small $(t - \tau)$, because the function $f(x, z)$, whose Fourier coefficients (a_{nk}) appear in this series, is very localized. This series may be resummed using the Poisson Summation Formula (Courant and Hilbert, 1953) to obtain a much more rapidly converging series suitable for numerical calculations. The result of this resummation is the solution

$$c(x, y, z, t) = \frac{1}{1+\beta} \cdot \int_0^t g(\tau)\, S_1(y, t-\tau)\, S_3(x, z, t-\tau)\mathrm{d}\tau, \quad (14)$$

where

$$S_3(x, z, t-\tau) = \frac{1}{4}\int_{-x_0}^{x_0}\mathrm{d}x' \int_{-z_0}^{z_0}\mathrm{d}z' f(x', z') \cdot \left[\frac{e^{-[(z-z')^2+(x-x')^2]/4\sigma(t-\tau)}}{4\pi\sigma(t-\tau)} \cdot \sum_{\mu=-\infty}^{\infty}\left\{e^{-x\delta[\mu^2-\mu(x+x')/x_0+xx'/x\delta]/\sigma(t-\tau)} + e^{-x\delta[\mu^2-\mu(x'-x)/x_0]/\sigma(t-\tau)}\right\} \cdot \sum_{\nu=-\infty}^{\infty}\left\{e^{-z\delta[\nu^2-\nu(z+z')/z_0+zz'/z\delta]/\sigma(t-\tau)} + e^{-z\delta[\nu^2-\nu(z'-z)/z_0]/\sigma(t-\tau)}\right\}\right] \quad (15)$$

and $\sigma = D/(1 + \beta)$ is the effective diffusion coefficient. It is the possibility of carrying out this resummation for both the x and z series that led us to use a rectangular cross-section for our domain. In the analogue of Eq. 8 for a circular cylinder, the r and θ series do not decouple, so only the z series may be resummed. In using Eq. 14, we explicitly assume that the channels are points, so that $f(x, z)$ is a sum of delta functions. Thus, $S_3(x, z, t, \tau)$ becomes a sum, over the channels (x_j, z_j) in our patch, of the expression within the large square brackets in Eq. 15 (x', z') is replaced by (x_j, z_j). For numerical calculation using the formula, the time integral is evaluated using Gaussian Quadrature (Atkinson, 1978), and each series is truncated at a term beyond which preliminary calculations indicated that the remainder would be much smaller than the numerical integration error.

In both one- and three-dimensional models, facilitation (F) of a response (R_2) is measured as its fractional increase compared with an unfacilitated response (R_1), $F = R_2/R_1 - 1$.

RESULTS

One-dimensional Model

Tetanic Facilitation. Fig. 2 *A* shows predictions of facilitation of synaptic responses to successive spikes in a train of 100 action potentials at 20 Hz. In performing these simulations, transmitter release was assumed to depend instantaneously on the square of the free submembrane calcium concentration (Charlton et al., 1982; Zucker, 1982; Zucker and Stockbridge, 1983). The decay of facilitation that would be seen by responses to single test action potentials at various intervals after the tetanus is also shown as the falling phase of the upper curve in Fig. 2 *A*. This may be compared to the decay of facilitation following a single action potential, also shown in Fig. 2 *A*. The decay of facilitation following the tetanus and a single impulse are shown on a faster time scale in Fig. 2 *B*.

Several properties of facilitation are evident from this simulation: (*a*) Facilitation declines with fast and slow components. When plotted on a 50-ms time scale, the decay of facilitation following a spike (Fig. 2, curve 5) can be described roughly as the sum of two exponentially decaying components, one with a time constant of ~5 ms and a magnitude of about 0.8 (Fig. 2, line 7), the second with a time constant of ~100 ms and magnitude of about 0.25 (Fig. 2, line 6). These are similar to the experimentally measured properties of facilitation at squid giant synapses (Charlton and Bittner, 1978). (*b*) Following a tetanus, facilitation (Fig. 2, curve 1) declines with similar phases (Fig. 2, lines 3 and 4) plus a third slower phase (Fig. 2, line 2), having a time constant of several seconds and a magnitude of about 1.5. (*c*) Facilitation to successive spikes rises rapidly at first, and then continues to grow slowly. The growth of facilitation has components similar to those of its decay. (*d*) The faster components of facilitation rise to a level of about 3 at the end of a tetanus. The latter three properties are difficult to measure at the squid giant synapse, due to the dominance of depression in such tetani (Kusano and Landau, 1975), but they are similar to the properties of tetanic facilitation reported at neuromuscular junctions (Mallart and Martin, 1967; Magleby, 1973; Magleby and Zengel, 1976; Magleby and Zengel, 1982). Thus the one-dimensional calcium diffusion model is reasonably successful in predicting the characteristics of tetanic facilitation and its posttetanic decay.

Presynaptic Average Free Calcium. The predicted rise of the total number of free calcium ions inside the terminal during a tetanus, and its subsequent decline, are plotted in Fig. 2 *C*. This may be compared to the change in average free cytoplasmic calcium measured spectrophotometrically with arsenazo III (Charlton et al., 1982). The simulated tetanic total calcium rises with a slightly declining slope to a peak of ~1 μM, similar to the experimental order-of-magnitude measurement of ~3 μM for similar tetani. Posttetanically, total calcium declines

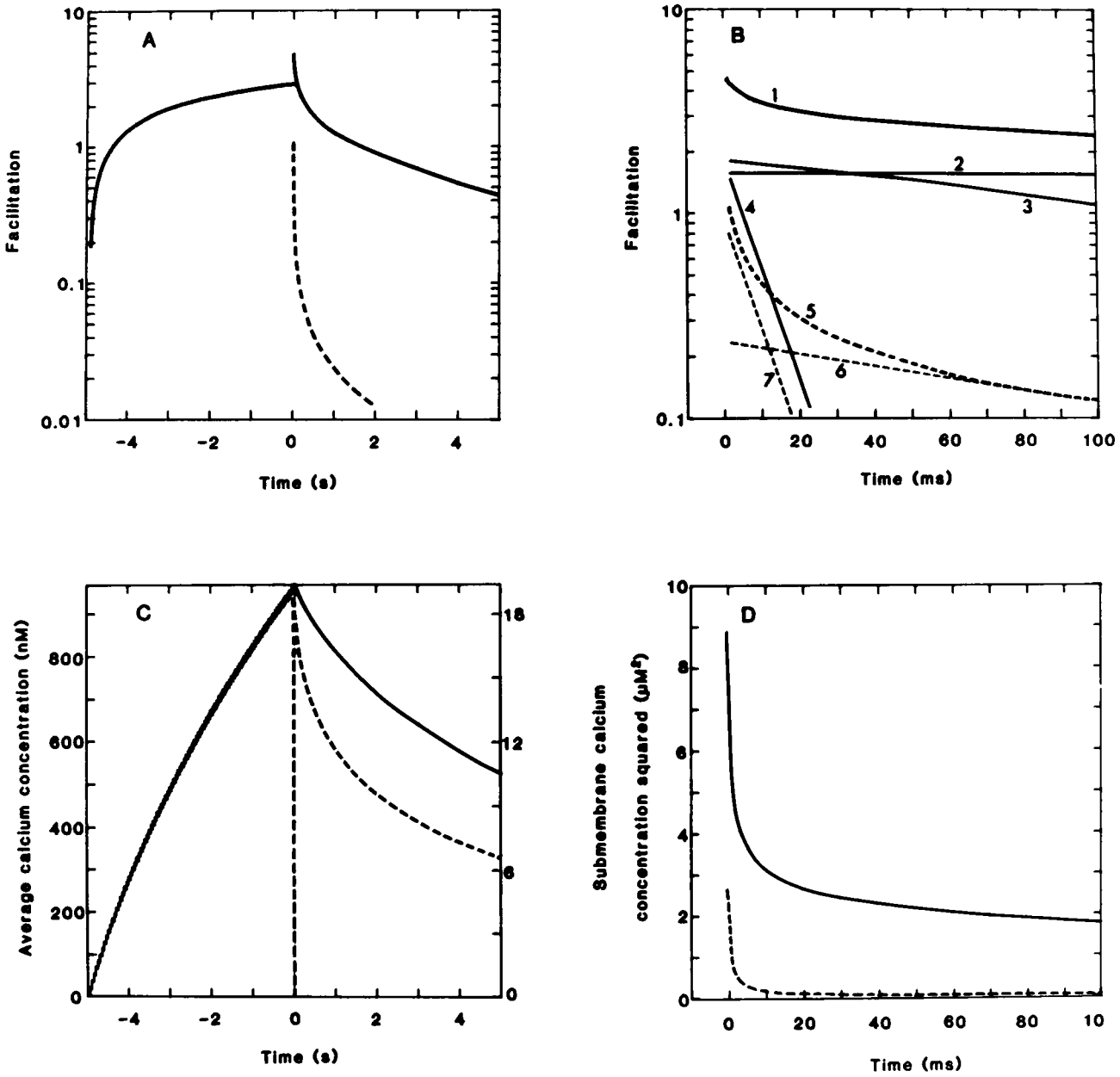

FIGURE 2 Simulations of synaptic transmission at squid giant synapse, using one-dimensional model and assuming two calcium ions cooperate to release a quantum of transmitter. In all panels, tetanic simulations are plotted as solid lines and single spike simulations as dashed lines. (*A*) Growth of facilitation to successive spikes in a tetanus (20 Hz, 5 s) and decay of facilitation measured at various intervals after the end of the train (at time 0) or after a single spike. Facilitation is the fractional increase in transmitter released by a tetanic or posttetanic spike, compared to release by a single spike. (*B*) Decay of posttetanic (curve 1) and postspike (curve 5) facilitation on a faster time scale. The decays have been decomposed into a series of exponentials (posttetanic: lines 2–4; postspike: lines 6 and 7) by peeling successive components, slowest first. (*C*) Change in average presynaptic free calcium concentration during a tetanus and one spike, normalized to the same peak. Left ordinate refers to tetanic response, right ordinate to single spike response. (*D*) Decay of square of active calcium (phasic transmitter release) following last spike in a tetenus (solid curve) and a single spike (dashed curve).

with a half-time of ~7 s, similar to experimental results. The simulated total calcium decays somewhat more slowly than that following a single spike, because in a tetanus calcium has diffused further from the membrane and so takes longer to be extruded at the membrane than does calcium that has entered during a single action potential. Unfortunately, the measurement of the decay of total calcium after one action potential is too crude to determine whether this aspect of the simulation is observed experimentally.

Time Course of Transmitter Release. Fig. 2 *D* illustrates the decline in simulated transmitter release for one spike and following the last spike in the tetanus. At the end of one action potential, active calcium reaches 1.53 μM. Phasic release evoked by one action potential drops to

10% of its peak in 4 ms. As expected, this is somewhat faster than the postsynaptic current declines (Charlton et al., 1982), a result of the kinetics of closing of the postsynaptic channels. However, the tetanic simulation predicts that even 100 ms after the last spike, transmitter release is occurring at nearly the same level as at the peak for the first spike. This is because residual calcium after a tetanus decays very slowly because of the reduced spatial calcium gradient after prolonged calcium influx, and so residual calcium remains a large fraction of the peak calcium reached in a single spike. Residual calcium is 1.35 μM at 100 ms after the last spike, 0.76 μM at 1 s, and 0.41 μM at 5 s after the end of the tetanus. This aspect of the model is independent of the relation assumed between transmitter release and active calcium. It predicts a continual release of transmitter for ~50 ms after the tetanus at a higher level than that at the peak of the first spike. Such behavior has never been observed at any chemical synapse, and is the crucial point of failure of the one-dimensional model.

Calcium Uptake. Various alternative formulations of the one-dimensional model have been devised and used to simulate tetanic facilitation, time course of transmitter release, and total free presynaptic calcium. For example, calcium could be removed not at the surface, but everywhere throughout cytoplasm by a first-order uptake mechanism, such as is reported for mitochondria and endoplasmic reticulum. Mitochondria take up calcium too slowly to account for the observed decline of presynaptic calcium (Brinley et al., 1978), but uptake into endoplasmic reticulum occurs with a time constant of seconds (Blaustein et al., 1978), similar to that observed at squid synapses. Such an uptake system accounts as well as does a surface pump for the tetanic arsenazo measurements. With internal uptake, unlike surface extrusion, presynaptic calcium declines at the same rate following one spike or a tetanus. As mentioned above, the experimental data are insufficient to distinguish these alternatives. Tetanic facilitation and the transmitter release following one or tetanic spikes behave similarly for both forms of calcium removal: facilitation is still well described, while posttetanic transmitter release persists too long.

Saturable Buffers. A second variant of the one-dimensional model that we considered was to allow the cytoplasmic buffer to saturate. Versions with 500 μM of a low-affinity buffer (K_D = 20 μM, cf. Alemà et al., 1973), or with 40 μM of a high affinity buffer (K_D = 100 nM, see Baker and Schlaepfer, 1978), or with both buffers present simultaneously, have been simulated. In these simulations, the diffusion equation and corresponding difference equations were modified as described by Barish and Thompson (1983). We found that neither type of saturable buffer substantially affected the time course of tetanic facilitation. The peak submembrane calcium concentrations reached in action potentials were much higher when saturable buffers were present, especially in the case of a high-affinity, low-capacity buffer, and the phasic decay of submembrane calcium occurred about twice as fast. Residual calcium, on the other hand, was little affected. Facilitation, which depends on the ratio of residual to peak calcium, was therefore reduced.

The most interesting result of the simulations using saturable buffers appeared in the total calcium predictions. A high-affinity, low-capacity buffer caused the total calcium signal to display a sharp drop to 50% in 2 ms, and a further rapid decline to 25% in 20 ms, due to the diffusion of unbound calcium past saturated submembrane buffer to unsaturated buffer where it was bound (see Connor and Nikolakopoulou, 1982). The kinetics of arsenazo's response to calcium might be too slow (see Discussion) to detect the initial 2-ms spike in the total calcium signal, but it should report most of the subsequent large drop in free calcium in the next 20 ms. Since no such decline in the arsenazo signal is seen (Charlton et al., 1982), the existence of a high-affinity, low-capacity buffer may be questioned. Brinley (1978) gives other reasons to doubt the presence of such a highly saturable buffer.

Three-dimensional Model

The chief failure of all versions of the one-dimensional model is that residual active calcium after a tetanus remains higher than the peak active calcium reached in the first spike for almost 100 ms after the end of the tetanus. We expected that near points of calcium entry through discrete channels, where transmitter release must occur (see Introduction), the peak calcium reached after each action potential must be much higher than predicted by a model of calcium entering uniformly across the surface. To test this idea, we developed the three-dimensional model of calcium entering through discrete channels. We assume that the channels open nearly simultaneously during the rising phase of the action potential, and remain open for exactly 1 ms before closing, and do not reopen in an action potential. Since the average channel lifetime is ~1 ms, similar to the duration of total calcium current (Llinás et al., 1982; Lux and Brown, 1984), these seem reasonable approximations.

Disposition of Calcium Channels. We must decide where to put the calcium channels and transmitter release sites in our model. Pumplin et al. (1981) found that contact between presynaptic and postsynaptic cells at the squid giant synapse occurs at active zones, which are roughly circular patches 0.65 μm^2 in area. The total area of synaptic contact ranged from 3,700 to 13,000 μm^2. Each of the approximately 10,000 active zones contained about 1,000 randomly scattered intramembranous particles, which are thought to correspond to calcium channels. The likely number of calcium channels to open in an action potential is far fewer than the total of 10^7 particles,

however. The calcium current in an action potential is ~240 nA for 1 ms (Llinás et al., 1982). If the single channel current during the action potential (at ~0 mV) is ~0.4 pA (Lux and Brown, 1984), then only 600,000 calcium channels, or 6% of the number of particles thought to represent calcium channels, open in a spike.

Fig. 1 *A–C* show how this distribution of calcium channels in active zones was represented in most of our simulations. Active zones consisted of square patches, 0.8 μm on a side, and containing 64 channels each in a square array, with 108 nm between calcium channels opened during an action potential. The 9,464 active zones were arranged in a square pattern of 26 by 364 zones over the face of the presynaptic terminal (50 μm × 700 μm) in contact with the postsynaptic axon. Each active zone was in the center of a square region of membrane 1.93 μm on a side, which was one face of an element of the terminal in which the diffusion equation was solved. The element was a rectilinear rod, 1.93 μm on a side and 50 μm long, extending through the cytoplasm to the opposite surface of the terminal. Calcium entered through the 64 open channels as point sources in the synaptic face, and was removed from the front and back surface of each element. By symmetry, there would be no net diffusion of calcium across the sides of the elements to neighboring identical elements. If it is also assumed that there is no diffusion or removal of calcium across the sides of the elements on the edge of the terminal, i.e., across the sides and ends of the terminal, then all elements will behave identically. Otherwise, edge zones would behave somewhat differently. Since only 8% of the active zones are on the edge, they will contribute little to synaptic transmission.

Location of Active Calcium Eliciting Release. Synaptic vesicles are also clustered at active zones (Pumplin and Reese, 1978). As explained in the Introduction, the short synaptic delay suggests that transmitter release occurs within ~50 nm of open calcium channels. We imagine that transmitter release occurs at specific vesicle attachment sites, which, like calcium channels, are integral membrane proteins. These proteins, ~5 nm in radius, must be separated by at least 10 nm. If vesicle fusion and exocytosis are to occur without displacing calcium channels, then vesicles with a 30 nm radius would have to fuse at least 35 nm from a calcium channel. We therefore imagine that the relevant active calcium concentration that acts to release transmitter is the submembrane free calcium concentration ~50 nm from calcium channel mouths opened during action potentials. This is similar to the spacing between sites of vesicle fusion and intramembranous particles thought to represent calcium channels at frog neuromuscular junctions (Heuser et al., 1979).

Prediction of Active Calcium in a Tetanus. Fig. 3 *A* shows the submembrane calcium at the center of an active zone, equidistant from the four centermost open calcium channels. After one spike, active calcium drops from a peak of 30 μM to ~2 μM in 10 ms. Fig. 3 *B* shows the peak active calcium concentration at the end of each spike and the calcium concentration just before each spike in a 5-s tetanus of 100 action potentials at 20 Hz. The posttetanic decay of residual active calcium is also shown. The values of pump rate (P), binding ratio (β), and total calcium influx in an action potential are the same as in the one-dimensional simulation. It is evident that the residual calcium after a tetanus, or before the last spike in a tetanus, is now much less than the peak calcium in the first spike. The reason is that the peak active calcium after one spike is nearly 20 times as big as that predicted if calcium enters uniformly across the entire presynaptic membrane. Active calcium drops very rapidly after each spike, diffusing in three dimensions away from channel mouths, until submembrane equilibrium is established. Then residual calcium drops much as it did in the one-dimensional model, due to radial diffusion into the interior of the terminal. It is now a much smaller fraction of peak active calcium in a spike than it was in the one-dimensional simulation.

Choice of Calcium Power Governing Release. To convert active calcium to transmitter release or predict synaptic facilitation, we need the relation between calcium and release. It is clear that with residual calcium now a smaller fraction of peak calcium in a spike, there will be less facilitation than in the one-dimensional simulation, or than is observed experimentally. To compensate for this reduction in relative residual calcium, a higher stoichiometry is needed for the reaction of calcium with release sites to release transmitter. Our simulations with the one-dimensional model assumed a stoichiometry of 2, based on measurements of the relationship between transmitter release and calcium current in voltage-clamp experiments (Charlton et al., 1982). More recent measures suggest powers of 3 or more (Smith et al., 1985). The dependence of transmitter release on external calcium also shows a power law dependence with exponents of from 2 to greater than 4 in different specimens (Katz and Miledi, 1970; Lester, 1970). Parnas et al. (1982) and Barton et al. (1983) have shown that this measurement is likely to underestimate the true stoichiometry of the reaction. Preliminary calculations (Zucker and Fogelson, 1986) indicate that the release vs. calcium-current relation also underestimates the calcium-release stoichiometry. We have chosen a value of $n = 5$ in our simulations with the three-dimensional model, which produces a facilitation similar to that observed experimentally.

Simulated Facilitation, Time Course of Release, and Total Calcium. Fig. 3 *C* and *D* show the tetanic growth, posttetanic decay, and postspike decay of facilitation on two time scales. Facilitation behaves very much as in the one-dimensional simulation (Fig. 2 *A* and *B*) and as reported experimentally (Charlton and Bittner, 1978). The

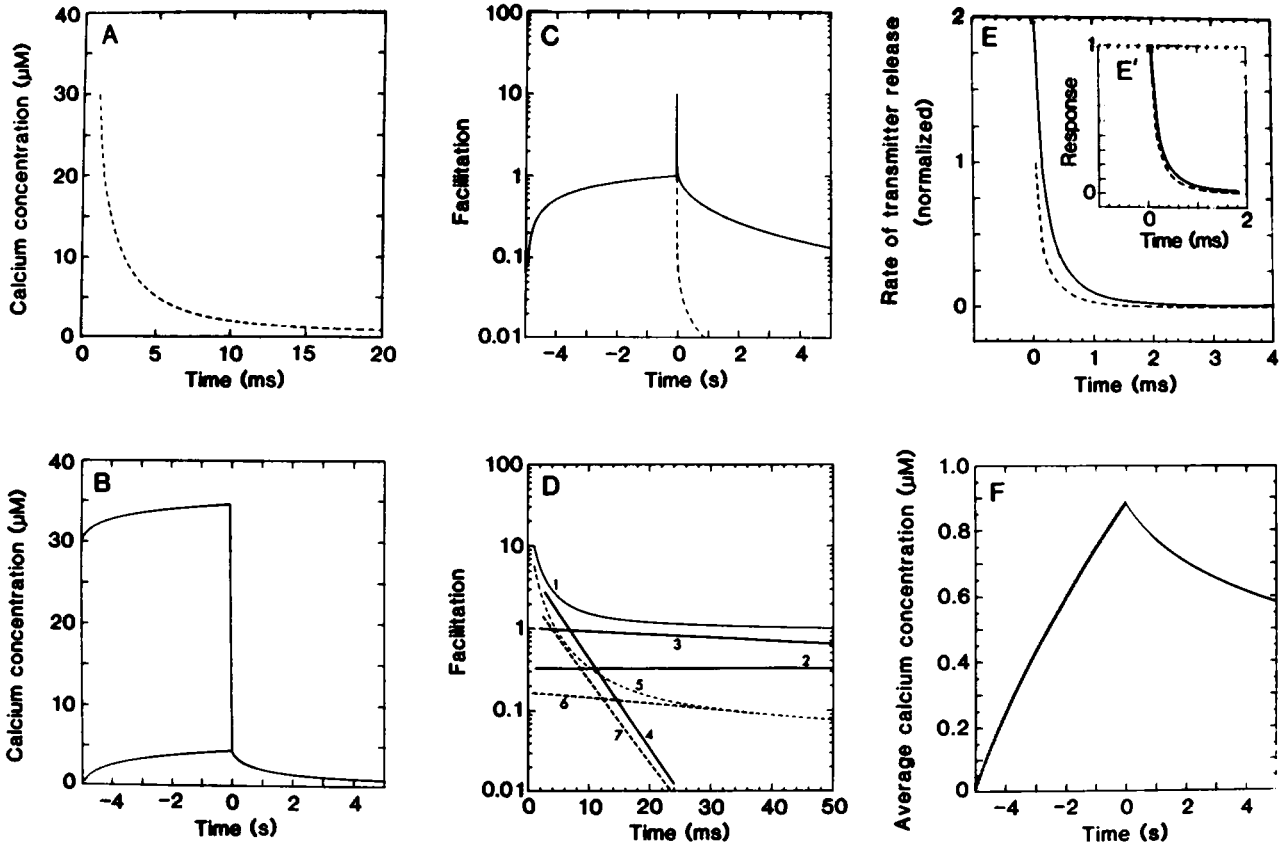

FIGURE 3 Simulations of synaptic transmission at squid giant synapse using three-dimensional model. A calcium cooperativity of 5 is assumed in Figs. 3–5. Transmitter release sites and calcium channels are located in active zone patches of presynaptic membrane. (*A*) Decay of active calcium following one spike. (*B*) Upper curve connects peaks of active calcium in successive spikes in a tetanus (20 Hz, 5 s) and subsequent decay of active calcium at end of tetanus (at time 0). Lower curve connects troughs of active calcium just before each successive spike. (*C*) Growth and decay of tetanic (solid curve) and decay of postspike (dashed curve) facilitation on a slow time scale. (*D*) Decay of posttetanic (solid curve) and postspike (dashed curve) facilitation on faster time scale and their exponential components (numbers as in Fig. 2 *B*). (*E*) Decay of fifth power of active calcium (phasic transmitter release) following last (solid curve) and first (dashed curve) tetanic spikes. Ordinate normalized to peak of first spike (equal to 1). In *E'*, the two curves are normalized to the same peak, to show differences in time course. (*F*) Average presynaptic calcium concentration during and after a tetanus.

early decay of facilitation (Fig. 3, curves 1 and 5) has rapid (5.7 ms, Fig. 3, lines 4 and 7) and slow (66 ms, Fig. 3, lines 3 and 6) components following either a tetanus or one spike, with a combined magnitude of 3 measured at an interval of 2 ms after 1 spike. There is an even briefer component of intense facilitation, corresponding to that measured experimentally by prolonging the depolarization of terminals (Katz and Miledi, 1968). Although not explicitly illustrated in Fig. 3 *D*, this component is evident from the fact that the initial amplitudes of the two illustrated components of facilitation (Fig. 3, lines 6 and 7) sum to less than the initial magnitude of facilitation (Fig. 3, curve 5). A slow component of facilitation (Fig. 3, line 2), with a decay constant of 7 s and magnitude 0.32, appears during and after a tetanus. Thus, tetanic facilitation accumulates in a tetanus in the three-dimensional model much as it does in the one-dimensional model. It is difficult to measure facilitation in isolation at squid giant synapses to long tetani. Charlton and Bittner (1978) report that facilitation rises within five spikes at 100 Hz to a plateau level of 0.5–1.0. We have also simulated brief trains at 100 Hz, and our fifth spike exhibited a facilitation of 0.804.

Fig. 3 *E* shows the predicted time course of active calcium raised to the fifth power for the first and last spike in the tetanus. Clearly, there is now little difference between these two spikes. If the change in active calcium is the rate limiting step in transmitter release, this should resemble the time course of release and be faster than the decay of postsynaptic current. In fact, the time course of release is similar to this at frog neuromuscular junctions (Barrett and Stevens, 1972), and postsynaptic current at squid giant synapses is slower than the predicted release function (Charlton et al., 1982).

We have predicted the arsenazo signal, indicating total free calcium, by calculating the total calcium influx minus total calcium efflux across the surface at each time, then integrating this net flux over time to get the total calcium in the cell, and dividing by the binding ratio and the volume to get the average free calcium concentration. The three-dimensional model (Fig. 3 *F*) behaves much like the one-

dimensional model (Fig. 2 *C*), and the simulations resemble experimental results (Charlton et al., 1982).

Submembrane Calcium at Different Locations. Fig. 3 deals with the submembrane calcium at the center of an active zone, 76 nm from each of four open calcium channels. We have also looked at the submembrane calcium at various distances from a channel located near the center of an active zone. Between 4 and 76 nm from such a calcium channel, the form and magnitude of the calcium transient are similar (differing by <3%) for both single spikes and a tetanus. This is because, by the end of a 1 ms influx, calcium has already diffused away from channel mouths, and the submembrane calcium is nearly uniform in the center of an active zone.

We have also computed the submembrane calcium near channels at various positions in an active zone. For release sites within three rows of the center of an active zone (eight-by-eight rows of channels), the peak calcium reached in both the first and last spike in a tetanus, and the rate of decay of residual calcium, are all within 5% of the values at the center of the active zone. Thus, 50% of the activated channels evoke release in a way nearly identical to those at the center (Fig. 3). Outside of this region, calcium concentrations are sufficiently lower that they are not well represented by Fig. 3 *A* and *B*. Between the outer two rows of channels, the peak calcium concentration for either the first or the last spike in a tetanus reaches 75–90% of the value for the center of the patch (less near a corner than at the middle of a row). It follows from the nonlinear dependence of release on active calcium that these and more peripheral release sites (beyond the outer row of channels) contribute little to synaptic transmission.

Effect of Channel Clustering. Why are calcium channels and transmitter release sites clustered into active zone patches? Would transmission be the same if the release machinery were distributed uniformly over the presynaptic surface that is in contact with the postsynaptic membrane? We approached these questions by considering the synapse's behavior for each of three configurations of synaptic machinery: In the first, 600,000 calcium channels are distributed uniformly in the synaptic face of the presynaptic terminal. The diffusion element of the terminal is now a slab, with nonsynaptic and synaptic faces of 50 μm × 242 nm and a length of 50 μm, containing 206 channels in a single row (Fig. 1 *D*). In the second configuration, the 600,000 channels are concentrated into a strip running longitudinally along the middle of the synaptic face and having an area of 7,000 μm^2, the same as the total area of active zones used in Fig. 3. This time, the diffusion element is a slab with dimensions of 50 μm × 108 nm on the synaptic face and a length of 50 μm, which contains a central 10 μm long row of 92 channels (Fig. 1 *E*). The third configuration has the channels clustered in active zones as described above (Fig. 1 *B*).

In Fig. 4 the behavior of these three distributions of synaptic machinery is compared. Each row illustrates active calcium and synaptic facilitation during a tetanus, and time course of release for the first and last spikes in the tetanus. In Fig. 4 *A*, the solid lines show simulations in which channels are dispersed uniformly throughout the synaptic face 242 nm apart in a square array. We illustrate simulations at 50 nm from a channel mouth. Similar results were obtained between 5 and 50 nm from the nearest channel, so that the precise location of vesicle fusion within the characteristic diffusion distance from channel mouths is not critical. The dashed lines show simulations at a point midway between (54 nm from each of) two channels in a row for the case of channels concentrated in a single synaptic strip with the same density as in active zones. Again, very similar results were observed at the edge of an element, 76 nm from each of four channels, or as close as 5 nm to a channel mouth. Similar results were also obtained near all but the outer two channels in the 92 lines of channels in the synaptic strip. Finally, the solid lines in Fig. 4 *B* illustrate simulations 76 nm from each of four channels when channels are clustered in active zones. As mentioned previously, similar results were obtained at points between 4 and 76 nm from channels not at the edge of an active zone. Thus the results are truly representative of the behavior of submembrane calcium at likely points of vesicle fusion near the majority of calcium channels for all three channel arrays. In all these simulations, $\beta = 40$ and $P = 0.02$ μm/ms.

Several differences are evident among the three arrays: Peak active calcium in a spike rises from 8 μM for channels distributed uniformly in the synaptic face to just over 30 μM for channels concentrated in a single strip or in dispersed active zones. Active calcium decays fastest from uniformly distributed and widely dispersed channels. Evidently, concentrating channels increases the peak active calcium and slows the initial rapid decay as a result of the increased overlap of calcium diffusing from neighboring channels. With uniformly dispersed channels, a point which is 50 nm from one channel can be no nearer than 92 nm to a second channel, and the next nearest channels would be 247 nm away. Here, active calcium and transmitter release are dominated by one calcium channel. When channels are concentrated into a strip or active zones, it is impossible for a point to be >76 nm from a channel, and then the point is equidistant from four. This leads to higher peaks and slower decays.

Active calcium accumulates with several time constants during a tetanus and decays afterwards with similar time constants. This leads to similar multicomponent facilitations for all channel arrays. Concentrating the channels into a strip speeds the time constants and reduces the magnitude of facilitation. This is because, at late times, the strip acts on a larger scale like a line source from which calcium diffuses in two dimensions, while the widely dispersed channels act as a plane source from which

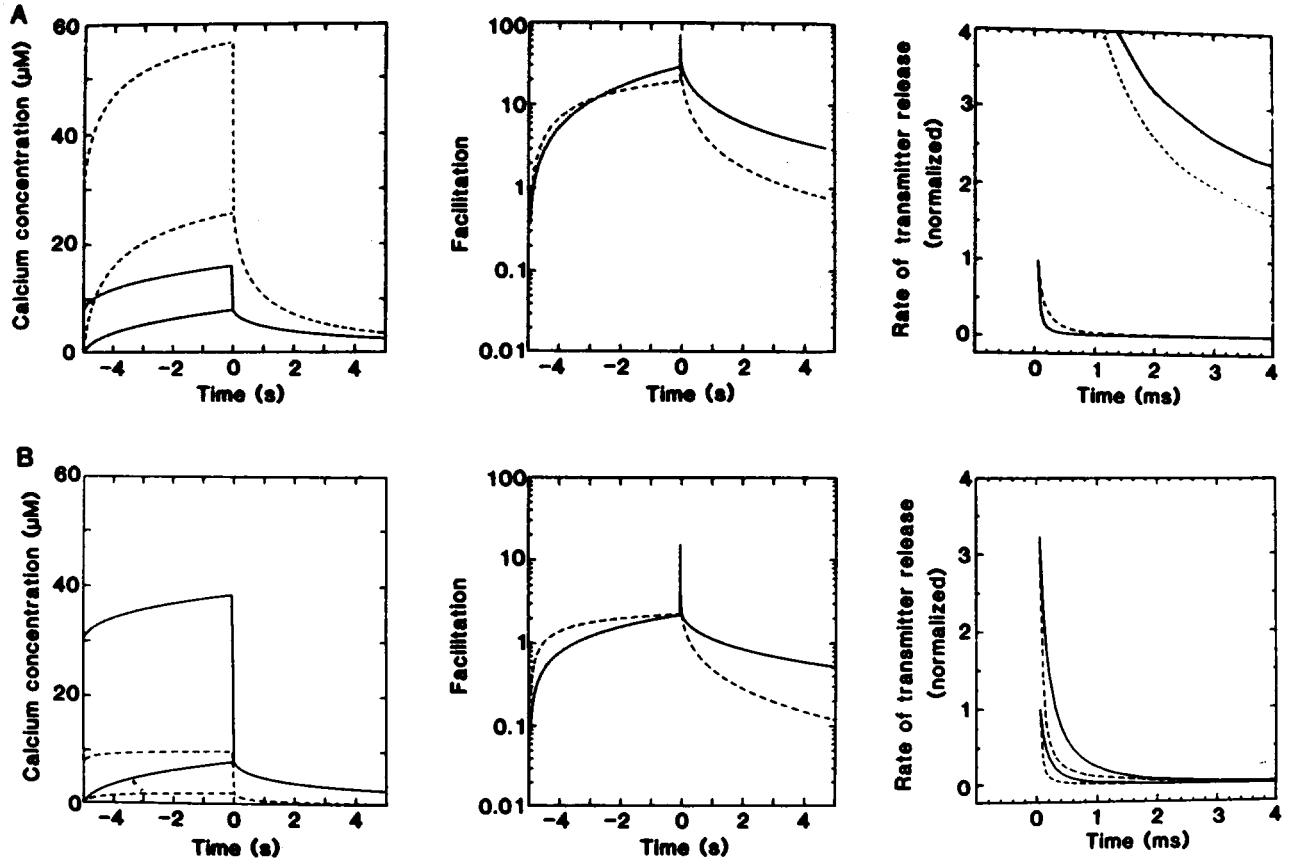

FIGURE 4 Effect of channel clustering and pump rate on synaptic transmission. Left column shows action potential peaks and pre-spike troughs of active calcium in a tetanus, and subsequent posttetanic decay. Middle column shows tetanic growth and posttetanic decay of facilitation. Right column shows phasic transmitter release following last spike (upper curve) and first spike (lower curve) in tetanus, normalized to peak of first spike. (*A*) Simulations in which calcium channels and release sites are dispersed throughout synaptic face (solid lines) or concentrated into a central strip (dashed lines). (*B*) Simulations in which calcium channels and release sites are clustered in active zones with the same density as in the strip (solid lines), and simulations in which release machinery is uniformly dispersed, but with a pump rate tenfold higher than in *A* (dashed lines).

diffusion is one-dimensional. The most interesting result, however, is that whether channels are uniformly dispersed or concentrated in a strip, posttetanic active calcium drops much too slowly to be consistent with the decay of transmitter release. This is the point of failure of the one-dimensional model. However, when channels are located in separated active zones, active calcium does dissipate rapidly enough after a tetanus. This is because each active zone acts at late times like a discrete disk source, from which calcium diffuses in three dimensions after each spike even on the larger scale. Hence, transmitter release decays almost as rapidly after the last spike in the tetanus as after the first spike, and tetanic facilitation is reduced to levels more consistent with experimental observation.

Effects of Buffer Ratio and Pump Rate. Another way to reduce residual calcium to levels consistent with a rapid decay of posttetanic transmitter release is to increase the pump rate (P). A 10-fold enhancement of pump rate (to 0.2 μm/ms) in the widely dispersed channel array leads to fast components of facilitation and time course of transmitter release (dashed lines in Fig. 4 *B*) similar to those for the active zone configuration of clustered channels. This increase in pump rate had little effect on the decay of active calcium following a single spike, but the slowest phase of facilitation (augmentation) was faster and less prominent.

We have also explored the effect of varying the ratio of bound to free calcium (β). Fig. 5 presents simulations using the active zone configuration of calcium channels, but with β set to 160 (solid lines) or 10 (dashed lines). In all cases, active calcium is measured midway between the central four channels in an active zone, and P = 0.02 μm/ms. Several effects are evident: Decreasing the proportion of calcium that is bound increases the peak active calcium. The increase is less than proportional to the change in β, because reducing β not only increases the proportion of entering calcium that remains free, but also speeds diffusion of calcium away from channel mouths, speeding the decay of transmitter release (if calcium activity is rate limiting). With β as high as 160, diffusion is sufficiently slowed that the peak in active calcium 76 nm from four

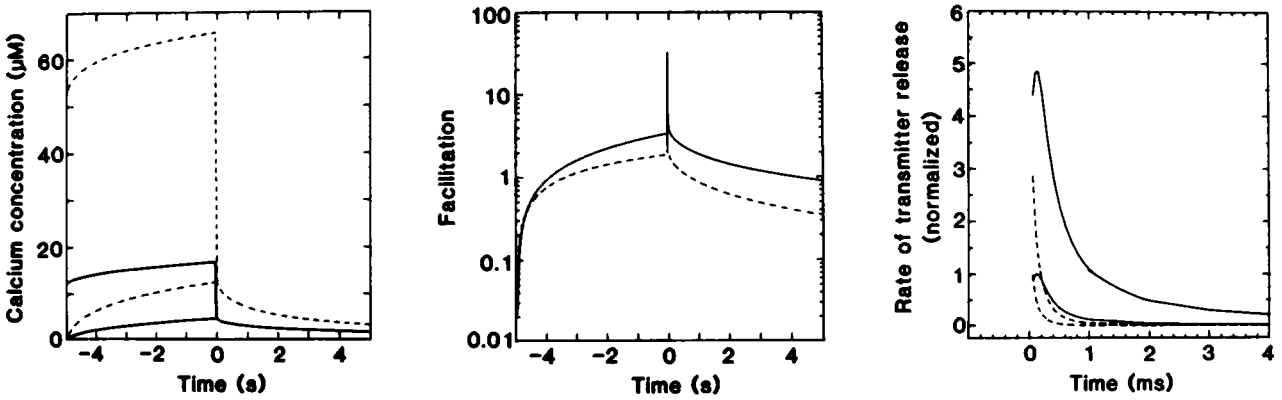

FIGURE 5 Effect of cytoplasmic calcium binding ratio on synaptic transmission. Active calcium in a tetanus, tetanic facilitation, and phasic release to first and last spikes are shown on left, middle, and right as in Fig. 4. The ratio of bound to free calcium is 160 (solid lines) or 10 (dashed lines). Calcium channels were clustered in active zones.

channels occurs a full millisecond after the end of the calcium influx. Thus, unlike changes in pump rate, changes in β have a large effect on the rapid early decay of active calcium following a spike.

The effect of reducing β on the slow component of calcium accumulation in a tetanus, and its posttetanic decay, is more complex. Reducing β is equivalent to increasing the pump rate in so far as extrusion is concerned. This is because the pump must compete with the calcium buffer for free calcium. Reducing β thus speeds removal of residual calcium, like increasing P, and results in less slow facilitation or augmentation. However, reducing β is less effective than increasing P, because reducing β also speeds diffusion. Calcium then moves more rapidly away from the surface to where it is less subject to pumping action.

Simulations of Frog Motor Neuron Terminals. Since it is not possible to observe synaptic facilitation without depression at the squid giant synapse in response to long tetani, we have adapted the three-dimensional diffusion model to frog neuromuscular junctions, where facilitation has been more thoroughly characterized. For this purpose, we chose as an element for calcium diffusion one active zone, 1 μm wide, in a long motor neuron terminal with a square cross section of 1.5 μm on a side (Fig. 1 *F* and *G*). Each active zone contains four rows of intramembranous particles thought to represent calcium channels (Heuser et al., 1979). These run perpendicular to the axis of the terminal in the synaptic face, and are located 25 and 35 nm, respectively, on either side of the centerline of the active zone. Synaptic vesicles release their contents ~50 nm lateral to each outer row of particles, so we concentrate on submembrane calcium at this distance from an outer row.

Since there are no measures of calcium binding, extrusion, uptake, or influx at motor nerve terminals, the choice of values for these parameters is somewhat arbitrary. We used values of β (100) and P (0.03 μm/ms) within the range of reported values for squid axons. Deciding the number of calcium channels opened by an action potential is more difficult. There are about 100 intramembraneous particles in each transverse row. If a similar proportion of these opens during action potentials as in the squid synapse, we would expect to have about six open channels per row, or 25 per active zone. We have tried simulations with from 10 to 80 channels per active zone.

In Fig. 6 *A* and *B*, we present simulations of active calcium after an action potential and during and after a tetanus. In this case there were three channels in the inner rows, and two in the outer rows, staggered and spaced 600 nm apart in each row (Fig. 1 *G*). Using a fourth-power relation between active calcium and transmitter release (Dodge and Rahamimoff, 1967), we predict the time course of transmitter release for the first and last spikes in the tetanus (Fig. 6 *C*), tetanic facilitation and its subsequent decay (Fig. 6 *D*), and the early postspike and posttetanic decay of facilitation. (Fig. 6 *E*).

Several results are remarkable: Active calcium rises to a peak of 7.8 μM in one spike, and 11.6 μM at the end of a 20-Hz, 5-s tetanus. Transmitter release evoked by the last spike drops to 25% of its peak at the end of the first spike in ~1 ms, so phasic release is preserved with only modest prolongation in a tetanus. Facilitation decays after a spike (Fig. 6, curve 4) and a tetanus (Fig. 6, curve 1) with fast (Fig. 6, lines 4 and 7) and slow (Fig. 6, lines 3 and 6) components of 10 and 266 ms, with magnitudes of 0.55 and 0.8 measured 3 ms after one spike. These facilitation properties are similar to those observed at frog neuromuscular junctions (Mallart and Martin, 1967; Magleby, 1973), except that measured facilitation decays initially somewhat more slowly than the simulations suggest (time constant of ~35–50 ms). As in the squid simulations, there is an early, brief, and intense phase of facilitation (not shown as a peeled component) corresponding to experimental observation (Katz and Miledi, 1968). During and after a tetanus, a very slow component of facilitation appears (Fig. 6, line 2), with a time constant of ~2.8 s and

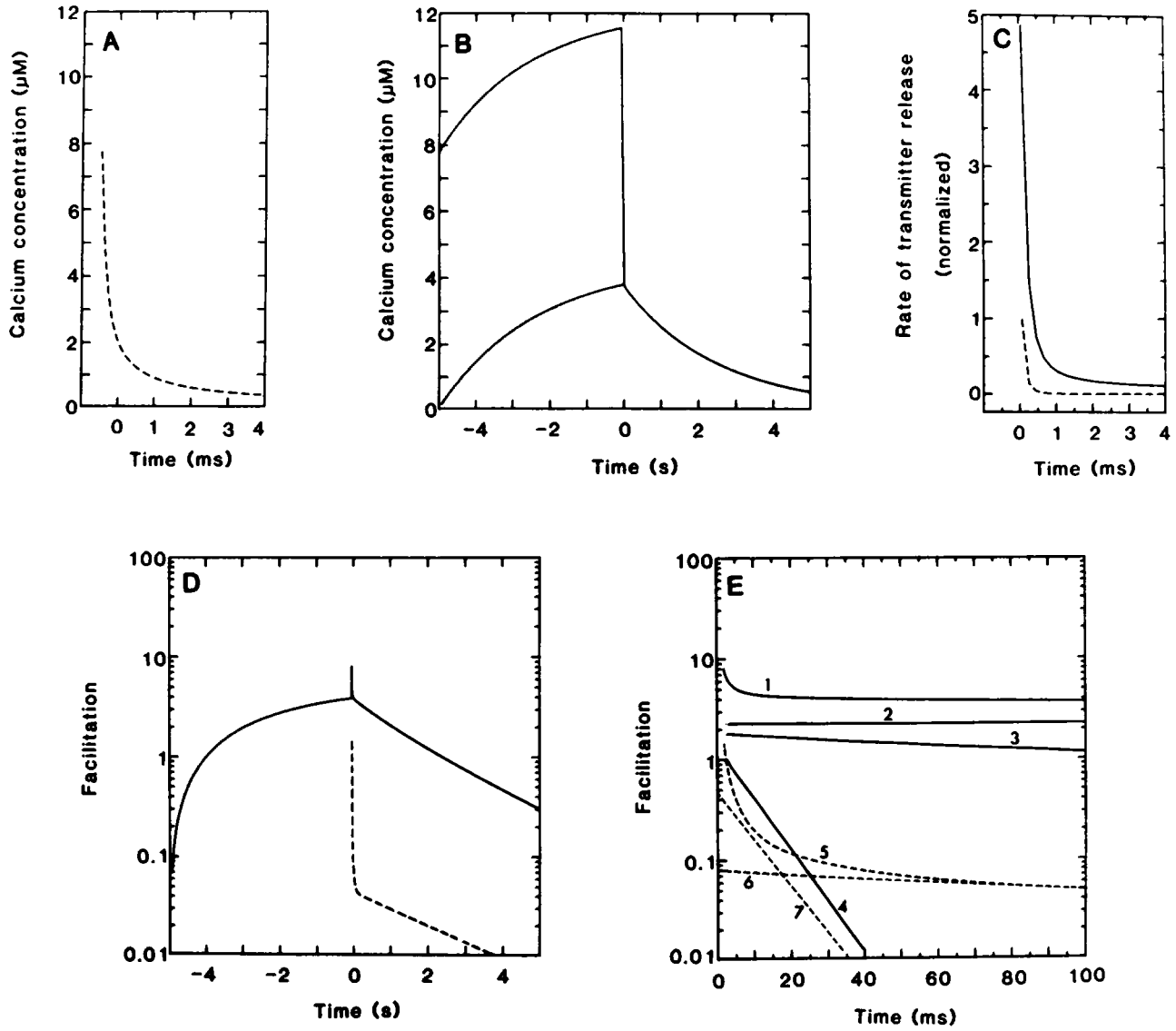

FIGURE 6 Simulations of synaptic transmission at frog neuromuscular junction, using three-dimensional model. A calcium cooperativity of 4 is assumed. (*A*) Decay of active calcium following one spike. (*B*) Peaks and troughs of active calcium in a tetanus and posttetanic decline of active calcium. (*C*) Phasic transmitter release following last (solid curve) and first (dashed curve) tetanic spikes, normalized to peak of first spike. (*D*) Tetanic and posttetanic (solid curve) and postspike (dashed curve) facilitation on a slow time scale, and their exponential components. (*E*) Posttetanic and postspike facilitation on a fast time scale (numbers as in Fig. 2 *B*).

magnitude of 2.5. This may be compared to augmentation at frog neuromuscular junctions, which has a time constant of 4–9 s and magnitude of 1–3 following a similar tetanus (Magleby and Zengel, 1976).

We are unaware of measurements of the time course of phasic release evoked by spikes late in a tetanus. Datyner and Gage (1980) recorded virtually identical time courses of release for the first through third spikes at 65 Hz. They saw only a slight (10%) prolongation of the foot of release, at one-tenth the peak. In our simulation of release to three spikes at this frequency (not illustrated) we also observed about a 10% prolongation of the foot at one-tenth the peak.

We have checked the dependence of the results on where we measure submembrane calcium in the line 50 nm lateral to the outer row of channels. Points opposite a channel in the outer row (50 nm away) or opposite a channel in the inner row (60 nm away) yield virtually identical results. In both cases, active calcium is dominated by influx from one channel, but influenced by diffusion from adjacent channels and from the nearest channel on the other side of the active zone. A point on the line of vesicles midway between channels in the inner and outer rows (~90 nm from each of two channels) reaches a peak calcium level 12% lower than opposite a channel, and so is 65% as likely to cause transmitter release. It makes little difference near which of the open channels in the active zone calcium is measured.

Increasing the number of open channels to between 5 and 20 in each row (20 and 80 per active zone) causes the active zone to behave more like a line source at late times. Augmentation and the slow components of facilitation then decay more rapidly. Due to the significant overlap of diffusion from adjacent channels, early release time course after a tetanus is slowed, dropping to only half the peak of the first spike in 2 ms. β and P can be adjusted to compensate for any one of these difficulties in simulations with higher channel densities, but only at the expense of worsening other aspects of the fit to observation. Thus, simulations with 10 open channels per active zone more closely resemble experimental data.

DISCUSSION

Accomplishments of the Simulations

Our study is hardly the first to treat transmitter release and synaptic facilitation as consequences of phasic and residual calcium. The experimental evidence that phasic release depends on calcium influx (Katz, 1969) and that facilitation and augmentation depend on calcium accumulation (Katz and Miledi, 1968; Rahamimoff et al., 1980; Charlton et al., 1982) is already quite strong. The interpretation of this evidence is not altered by the present simulations. Others have also argued that phasic release is kinetically driven by changes in active calcium (e.g., Llinás et al., 1981) and that facilitation and augmentation can be explained by residual active calcium and a high calcium-release stoichiometry (e.g., Parnas et al., 1982; Magleby and Zengel, 1982; Zucker and Lara-Estrella, 1983). What is unique about calcium diffusion models is that they attempt to predict the magnitude and time course of phasic and residual calcium from a consideration of physical and chemical processes known to regulate calcium in neurons.

A simple one-dimensional model (Zucker and Stockbridge, 1983; Stockbridge and Moore, 1984) predicts accurately the radial distribution of residual calcium after repetitive activity. However, it fails to predict the magnitude and time course of active calcium at transmitter release sites near calcium channel mouths right after action potentials. A more realistic three-dimensional model, in which calcium enters through discrete channels arranged in patterns suggested by ultrastructural observations, is more successful in predicting some characteristics of synaptic transmission. In particular, the three-dimensional model predicts that posttetanic residual calcium remains a fraction of the peak active calcium in a single spike. It yields reasonable levels of tetanic facilitation in frog and squid with a calcium-release stoichiometry of 4 or 5, consistent with experimental estimates. Such a degree of calcium cooperativity generates too much tetanic facilitation in the one-dimensional model. One surprising result is that with a realistic choice of calcium extrusion rate, calcium channels had to be clustered into separated active zones to keep residual calcium from accumulating too heavily near calcium channels. This may be why the synaptic machinery is clustered in this fashion.

Another difference between one- and three-dimensional models is that the latter predicts peak active calcium levels of >30 μM in late tetanic spikes in the squid, while the former predicts active calcium levels of only 3 μM. This has important implications for the sensitivity of the release machinery to calcium concentration. It might appear that an increase of active calcium of nearly 1,000 times from its resting level of $\sim$50 nM might reduce the driving force on calcium sufficiently to retard the calcium influx in late tetanic spikes. However, application of constant field theory to calcium channels indicates that the calcium current will be reduced by only 0.03% by this elevation of calcium near channel mouths.

Our simulations are not very stiff, in that fourfold changes in parameters such as buffer binding ratio, calcium pump rate, channel number or density, or distance of release sites from channel mouths affect quantitatively but not qualitatively the time courses and magnitudes of calcium accumulation, phasic transmission, and facilitation. With parameter values chosen to be consistent as much as possible with direct experimental measurements, the simulations resemble remarkably closely the dynamic properties of synaptic transmission at highly facilitating synapses, such as frog neuromuscular junctions.

Limitations of the Model

The fit to experiment is not perfect, however. For example, the slowest component of facilitation (augmentation) decayed with a time constant of 2.8 s, compared to a typically observed time constant of 7 s (Magleby and Zengel, 1976). Reducing the pump rate, or increasing the binding ratio, increases this time constant in our simulations, but then the predicted magnitude of augmentation is too high. The early component of facilitation in frog, measured beginning $\sim$5 ms after an action potential (the typical absolute refractory period), was $\sim$12 ms in our simulations, compared with an average of 35 ms observed experimentally. Finally, the tail of residual calcium shortly after a tetanus, although sufficient to account for facilitation, predicts a large increase in frequency of spontaneously released quanta of transmitter. This predicted increase in miniature postsynaptic potential frequency is observed at crayfish neuromuscular junctions (Zucker and Lara-Estrella, 1983), but not at those of frog (Zengel and Magleby, 1981).

Several other qualities of synaptic transmission are not explained by our model: (*a*) The time course of transmitter release has a high Q_{10} (Charlton and Atwood, 1979). At least at low temperature, it is clearly not a diffusion-limited process. Perhaps the dynamics of exocytosis determine the time course of transmitter release. We make no attempt to represent these dynamics in our model, nor to account for the form of the time course of phasic release and its synaptic delay. (*b*) We do not treat effects of changing

external calcium, magnesium, and temperature on phasic release and facilitation. Such effects could be due to influences on various processes (exocytotic machinery, calcium buffering, calcium extrusion, transmitter mobilization, etc.). Little information is available to choose between the alternatives, so their incorporation into our model is premature. (*c*) The evidence for a specific role of presynaptic membrane potential in regulating transmitter release (Llinás et al., 1981; Dudel et al., 1983) is treated critically in two separate publications (Zucker and Landò, 1986; Zucker and Fogelson, 1986). No such role is included in the present model.

These imperfections are proof that the model is not a complete and totally accurate representation of the processes controlling transmitter release. Many simplifying assumptions are certainly incorrect: uniform, nonsaturating, and instantly equilibrating calcium buffering, linear nonsaturable extrusion only at front and back surfaces, no internal uptake of calcium, and a simple nonsaturating power-law relation between calcium and transmitter release. The model includes no provision to account for synaptic depression, such as a limited, but refillable, releasable transmitter store. And there was no attempt to account for tetanic and posttetanic potentiation, which appear to depend on the presynaptic entry and accumulation of sodium ions (Rahamimoff et al., 1980). Possible effects of internal membrane surface charge on submembrane calcium concentration were also ignored. Thus, the present three-dimensional model must be regarded as only one step toward understanding some of the physical processes that determine some of the properties of transmitter release, and, in particular, an improvement over the one-dimensional model used heretofore.

One characteristic of our model is that the same calcium channels are assumed to open in successive impulses. Since channel activation is a stochastic process, and there appear to be many more submembrane particles or available calcium channels than open channels, this is an unrealistic assumption. This turns out not to matter, however, since by the time of a subsequent action potential the submembrane residual calcium has fully equilibrated throughout an active zone, so it makes no difference where in the active zone the next channels to open are located.

One serious limitation to our analytic solution of the diffusion equation in three dimensions is that it relies on linear solution methods. Thus, we cannot incorporate the effects of saturable extrusion and buffering, as we could in the one-dimensional model solved by numerical approximation methods. The inability to treat saturable and noninstantaneous buffers is particularly disappointing, because even a low-affinity, high-capacity buffer is likely to be saturated near calcium channel mouths, where the local increase in total (bound plus free) calcium is ~1 mM.

It is worth considering the probable consequences of such local buffer saturation: (*a*) If calcium buffers saturate near calcium channels, the local peak free calcium concentration will be even higher, whereas residual calcium will be unaffected (as shown by our simulations with the one-dimensional model). Consequently, facilitation will be reduced. This effect may be compensated by adjustment of the buffer ratio (β) or the pump rate (P). (*b*) A saturated buffer does not retard diffusion, so initial diffusion of calcium away from channel mouths will be even faster than in our simulations, until local calcium drops to levels below the buffer capacity. This makes the initial decay of active calcium, and phasic transmitter release, even faster. (*c*) In our simulations, raising β slowed facilitation but prolonged posttetanic time course of release. If calcium channels are surrounded by a particularly high buffer concentration (local high β), which is saturable, the rapid decay of calcium in a spike (above saturation levels) will be preserved, while the early component of facilitation will be slowed (due to higher β). This may be the reason why the decay of facilitation was too fast at early times in our simulations of frog neuromuscular junction. (*d*) Finally, a saturable buffer has implications for free calcium measurements using arsenazo. The diffusion of calcium from locally saturated to unsaturated buffer regions away from channel mouths will be accompanied by a rapid drop in total free presynaptic calcium (see Connor and Nikolakopoulou, 1982). However, it is unlikely that arsenazo will report this calcium spike accurately. The relaxation time constant for the reaction of arsenazo with calcium has been variously estimated as 2.5–30 ms (Scarpa et al., 1978; Ogawa et al., 1980; Dorogi et al., 1983). Unfortunately, none of these measurements were made under conditions of arsenazo concentration, ionic strength, magnesium concentration, or calcium buffering that prevail in cytoplasm, so the association and dissociation rates for calcium-arsenazo complexes may be substantially different under physiological conditions. Nevertheless, on present evidence one would expect arsenazo to respond to a true step in total free calcium (case of nonsaturable buffer) with an absorbance change that rises to a plateau in perhaps 10 ms. On the other hand, a spike of free calcium near channel mouths, arising from local buffer saturation, and lasting only ~1 ms, would be like an impulse so far as arsenazo is concerned, and would result in a step increase in absorbance decaying in ~10 ms. If there is a calcium concentration spike superimposed on a step, such as would occur with a saturable buffer, the signal's rising phase in response to the step might cancel the falling phase responding to the impulse, resulting in something like the plateau response observed (Charlton et al., 1982). In other words, the situation most consistent with arsenazo's reaction kinetics and the observed response is a spike in free calcium such as would occur with local calcium buffer saturation in the immediate region of calcium channel mouths. These considerations emphasize the primitive nature of both the present simulations and our ability to measure changes in presynaptic calcium affecting transmitter release.

Supported by National Institutes of Health grant NS 15114 and Department of Education contract DE-AC03-76SF0098.

Received for publication 15 February 1985 and in revised form 11 July 1985.

REFERENCES

Alemà, S., P. Calissano, G. Rusca, and A. Giuditta. 1973. Identification of a calcium-binding, brain specific protein in the axoplasm of squid giant axons. *J. Neurochem.* 20:681–689.

Atkinson, K. E. 1978. An Introduction to Numerical Analysis. John Wiley & Sons, Inc., New York. 231–243.

Baker, P. F., and W. W. Schlaepfer. 1978. Uptake and binding of calcium by axoplasm isolated from giant axons of *Loligo* and *Myxicola*. *J. Physiol. (Lond.)*. 276:103–125.

Barish, M. E., and S. H. Thompson. 1983. Calcium buffering and slow recovery kinetics of calcium-dependent outward current in molluscan neurones. *J. Physiol. (Lond.)*. 337:201–219.

Barrett, E. F., and C. F. Stevens. 1972. The kinetics of transmitter release at the frog neuromuscular junction. *J. Physiol. (Lond.)*. 227:691–708.

Barton, S. B., I. S. Cohen, and W. van der Kloot. 1983. The calcium dependence of spontaneous and evoked quantal release at the frog neuromuscular junction. *J. Physiol. (Lond.)*. 337:735–751.

Berg, P. W., and J. L. McGregor. 1966. Elementary Partial Differential Equations. Holden-Day, San Francisco. 14–111.

Blaustein, M. P., R. W. Ratzlaff, and E. S. Schweitzer. 1978. Calcium buffering in presynaptic nerve terminals. II. Kinetic properties of the nonmitochondrial Ca sequestration mechanism. *J. Gen. Physiol.* 72:43–66.

Brinley, F. J., Jr. 1978. Calcium buffering in squid axons. *Annu. Rev. Biophys. Bioeng.* 7:363–392.

Brinley, F. J., Jr., T. Tiffert, and A. Scarpa. 1978. Mitochondrial and other calcium buffers of squid axon studied *in situ*. *J. Gen. Physiol.* 72:101–127.

Chad, J. E., and R. Eckert. 1984. Calcium domains associated with individual channels can account for anomalous voltage relations of Ca-dependent responses. *Biophys. J.* 45:993–999.

Charlton, M. P., and H. L. Atwood. 1979. Synaptic transmission: temperature-sensitivity of calcium entry in presynaptic terminals. *Brain Res.* 170:543–546.

Charlton, M. P., and G. D. Bittner. 1978. Facilitation of transmitter release at squid synapses. *J. Gen. Physiol.* 72:471–486.

Charlton, M. P., S. J. Smith, and R. S. Zucker. 1982. Role of presynaptic calcium ions and channels in synaptic facilitation and depression at the squid giant synapse. *J. Physiol. (Lond.)*. 323:173–193.

Connor, J. A., and G. Nikolakopoulou. 1982. Calcium diffusion and buffering in nerve cytoplasm. *Lect. Math. Life Sci.* 15:79–101.

Courant, R., and D. Hilbert. 1953. Methods of Mathematical Physics. Interscience Publishers, New York. Vol 1. 75–77.

Datyner, N. B., and P. W. Gage. 1980. Phasic secretion of acetylcholine at a mammalian neuromuscular junction. *J. Physiol. (Lond.)*. 303:299–314.

DiPolo, R., J. Requena, F. J. Brinley, Jr., L. J. Mullins, A. Scarpa, and T. Tiffert. 1976. Ionized calcium concentrations in squid axons. *J. Gen. Physiol.* 67:433–467.

Dodge, F. A., Jr., and R. Rahamimoff. 1967. Co-operative action of calcium ions in transmitter release at the neuromuscular junction. *J. Physiol. (Lond.)*. 193:419–432.

Dorogi, P. L., C.-R. Rabl, and E. Neumann. 1983. Kinetic scheme for Ca^{2+}-arsenazo III interactions. *Biochem. Biophys. Res. Commun.* 111:1027–1033.

Dudel, J., I. Parnas, and H. Parnas. 1983. Neurotransmitter release and its facilitation in crayfish muscle. VI. Release determined by both, intracellular calcium concentration and depolarization of the nerve terminal. *Pfluegers Arch. Eur. J. Physiol.* 399:1–10.

Heuser, J. E., T. S. Reese, M. J. Dennis, Y. Jan, L. Jan, and L. Evans. 1979. Synaptic vesicle exocytosis captured by quick freezing and correlated with quantal transmitter release. *J. Cell Biol.* 81:275–300.

Katz, B. 1969. The Release of Neural Transmitter Substances. Charles C. Thomas, Publisher, Springfield, IL, 60 pp.

Katz, B., and R. Miledi. 1968. The role of calcium in neuromuscular facilitation. *J. Physiol. (Lond.)*. 195:481–492.

Katz, B., and R. Miledi. 1970. Further study of the role of calcium in synaptic transmission. *J. Physiol. (Lond.)*. 207:789–801.

Kusano, K., and E. M. Landau. 1975. Depression and recovery of transmission at the squid giant synapse. *J. Physiol. (Lond.)*. 245:13–32.

Lester, H. A. 1970. Transmitter release by presynaptic impulses in the squid stellate ganglion. *Nature (Lond.)*. 227:493–496.

Llinás, R. R. 1977. Calcium and transmitter release in squid synapse. *Soc. Neurosci. Symp.* 2:139–160.

Llinás, R., I. Z. Steinberg, and K. Walton. 1981. Relationship between presynaptic calcium current and postsynaptic potential in squid giant synapse. *Biophys. J.* 33:323–352.

Llinás, R., M. Sugimori, and S. M. Simon. 1982. Transmission by presynaptic spike-like depolarization in the squid giant synapse. *Proc. Natl. Acad. Sci. USA.* 79:2415–2419.

Lux, H. D., and A. M. Brown. 1984. Patch and whole cell calcium currents recorded simultaneously in snail neurons. *J. Gen. Physiol.* 83:727–750.

Magleby, K. L. 1973. The effect of repetitive stimulation on facilitation of transmitter release at the frog neuromuscular junction. *J. Physiol. (Lond.)*. 234:327–352.

Magleby, K. L., and J. E. Zengel. 1976. Augmentation: a process that acts to increase transmitter release at the frog neuromuscular junction. *J. Physiol. (Lond.)*. 257:449–470.

Magleby, K. L., and J. E. Zengel. 1982. A quantitative description of stimulation-induced changes in transmitter release at the frog neuromuscular junction. *J. Gen. Physiol.* 80:613–638.

Mallart, A., and A. R. Martin. 1967. An analysis of facilitation of transmitter release at the neuromuscular junction of the frog. *J. Physiol. (Lond.)*. 193:679–694.

Moore, J. W., F. Ramón, and R. W. Joyner. 1975. Axon voltage-clamp simulations. I. Methods and tests. *Biophys. J.* 15:11–24.

Ogawa, Y., H. Harafuji, and N. Kurebayashi. 1980. Comparison of the characteristics of four metallochromic dyes as potential calcium indicators for biological experiments. *J. Biochem. (Tokyo)*. 87:1293–1303.

Parnas, H., J. Dudel, and I. Parnas. 1982. Neurotransmitter release and its facilitation in crayfish. I. Saturation kinetics of release, and of entry and removal of calcium. *Pfluegers Arch. Eur. J. Physiol.* 393:1–14.

Pumplin, D. W., and T. S. Reese. 1978. Membrane ultrastructure of the giant synapse of the squid *Loligo pealei*. *Neuroscience.* 3:685–696.

Pumplin, D. W., T. S. Reese, and R. Llinás. 1981. Are the presynaptic membrane particles the calcium channels? *Proc. Natl. Acad. Sci. USA.* 78:7210–7213.

Rahamimoff, R., A. Lev-Tov, and H. Meiri. 1980. Primary and secondary regulation of quantal transmitter release: calcium and sodium. *J. Exp. Biol.* 89:5–18.

Scarpa, A., F. J. Brinley, Jr., and G. Dubyak. 1978. Antipyralazo III, a "middle range" Ca^{2+} metallochromic indicator. *Biochemistry.* 17:1378–1386.

Simon, S., M. Sugimori, and R. Llinás. 1984. Modelling of submembranous calcium-concentration changes and their relation to rate of presynaptic transmitter release in the squid giant synapse. *Biophys. J.* 45(2, Pt. 2):264*a*. (Abstr.)

Smith, S. J., G. J. Augustine, and M. P. Charlton. 1985. Evidence for cooperative calcium action in secretion of synaptic transmitter. *Proc. Natl. Acad. Sci. USA.* 82:622–625.

Stockbridge, N., and J. W. Moore. 1984. Dynamics of intracellular calcium and its possible relationship to phasic transmitter release and facilitation at the frog neuromuscular junction. *J. Neurosci.* 4:803–811.

Zengel, J. E., and K. L. Magleby. 1981. Changes in miniature endplate

potential frequency during repetitive nerve stimulation in the presence of Ca^{2+}, Ba^{2+}, and Sr^{2+} at the frog neuromuscular junction. *J. Gen. Physiol.* 77:503–529.

Zucker, R. S. 1982. Processes underlying one form of synaptic plasticity: facilitation. *In* Conditioning: Representation of Involved Neural Functions. C. D. Woody, editor. Plenum Publishing Corp., New York. 249–264.

Zucker, R. S. 1984. A calcium diffusion model predicts facilitation, but not the time course of transmitter release, during tetanic stimulation. *Biophys. J.* 45(2, Pt.2):264*a*. (Abstr.)

Zucker, R. S. 1985*a*. Synaptic facilitation and residual calcium. *In* Model Neural Networks and Behavior. A. I. Selverston, editor. Plenum Publishing Corp., New York. 461–475.

Zucker, R. S. 1985*b*. Calcium diffusion models and transmitter release in neurons. *Fed. Amer. Soc. Exp. Biol. Proc.* In press.

Zucker, R. S., and A. L. Fogelson. 1986. Relationship between transmitter release and presynaptic calcium influx when calcium enters through discrete channels. *Proc. Natl. Acad. Sci. USA.* In press.

Zucker, R. S., and L. Landò. 1986. Mechanism of transmitter release: voltage hypothesis and calcium hypothesis. *Science (Wash. DC).* In press.

Zucker, R. S., and L. O. Lara-Estrella. 1983. Post-tetanic decay of evoked and spontaneous transmitter release and a residual-calcium model of synaptic facilitation at crayfish neuromuscular junctions. *J. Gen. Physiol.* 81:355–372.

Zucker, R. S., and N. Stockbridge. 1983. Presynaptic calcium diffusion and the time courses of transmitter release and synaptic facilitation at the squid giant synapse. *J. Neurosci.* 3:1263–1269.